Int. J. Heat Mass Transfer. Vol. 20, pp. 867–875. Pergamon Press 1977. Printed in Great Britain

ANALYSIS OF MIXED FORCED AND FREE CONVECTION ABOUT A SPHERE

T. S. CHEN and A. MUCOGLU
Department of Mechanical and Aerospace Engineering, University of Missouri-Rolla, Rolla, MO 65401, U.S.A.

(*Received* 20 *September* 1976 *and in revised form* 5 *November* 1976)

Abstract—An analysis is performed to study the flow- and heat-transfer characteristics of laminar mixed forced and free convection about a sphere. The transformed conservation equations of the nonsimilar boundary layers are solved by a finite difference method. Numerical results for gases having a Prandtl number of 0.7 are presented for buoyancy parameters which cover the entire regime of mixed convection, ranging from pure forced convection to pure free convection. In general, it is found that both the local-friction factor and the local Nusselt number increase with increasing buoyancy force for aiding flow and decrease with increasing buoyancy force for opposing flow. The effects of the variation of the local free stream velocities on the wall shear and surface heat-transfer results are also examined. With respect to the heat-transfer results, the buoyancy force effects on forced convection become significant for $Gr/Re^2 > 1.67$ and < -1.33, respectively for aiding and opposing flows. The inertia force effects on free convection are found to be significant for $Re^2/Gr > 0.01$. The buoyancy-affected velocity profiles exhibit an overshoot beyond the local free stream velocity for aiding flow and an S-shape for opposing flow.

NOMENCLATURE

C_f, local friction factor [1];
F, reduced stream function [1], equation (26);
f, reduced stream function [1], equation (9);
g, gravitational acceleration [m/s^2];
h, local heat-transfer coefficient [W/m^2 K];
Gr, Grashof number, $g\beta(T_w - T_\infty)R^3/\nu^2$ [1];
k, thermal conductivity [W/mK];
Nu, local Nusselt number, hR/k [1];
Pr, Prandtl number [1];
q_w, local surface heat-transfer rate per unit area [W/m^2];
R, radius of sphere [m];
r, radial distance from symmetrical axis to surface [m];
Re, Reynolds number, $u_\infty R/\nu$ [1];
T, fluid temperature [K];
T_w, wall temperature [K];
T_∞, free stream temperature [K];
U, local free stream velocity [m/s];
u, velocity component in x direction [m/s];
u_∞, undisturbed oncoming free stream velocity [m/s];
v, velocity component in y direction [m/s];
x, y, dimensional coordinates shown in Fig. 3 [m];
X, Y, dimensionless coordinates [1], equation (25).

Greek symbols

α, thermal diffusivity [m^2/s];
β, coefficient of thermal expansion [K^{-1}];
η, pseudo-similarity variable [1], equation (8);
θ, dimensionless temperature [1], equation (9);
μ, dynamic viscosity [Ns/m^2];
ν, kinematic viscosity [m^2/s];
ξ, transformed axial coordinate [1], equation (8);
τ_w, wall shear stress [N/m^2];
Φ, dimensionless temperature [1], equation (26);
ϕ, angular coordinate [rad];
ψ, stream function [m^2/s];
Ω, buoyancy parameter, $|Gr|/Re^2$, [1];
Ω^*, forced flow parameter, $1/\Omega = Re^2/|Gr|$, [1].

Subscript

0, stagnation condition.

INTRODUCTION

LAMINAR heat transfer from a sphere has been the subject of numerous analytical and experimental investigations from the standpoint of either pure free convection or pure forced convection (see, for example [1–10]). The neglect of buoyancy force effects on forced convective heat transfer may not be justified when the velocity is small and the temperature difference between the surface and the ambient fluid is large. Thus, predictions of the local heat-transfer rate in the mixed convection regime are of practical interest, as are the conditions under which the buoyancy-force effects first become significant.

The problem of mixed forced and free convection about a sphere has received relatively little attention. To the best knowledge of the authors, the only such studies which have been reported are the experimental work of Yuge [11] and Klyachko [12] and the analytical work of Hieber and Gebhart [13]. These studies, both experimental and analytical, were conducted under the conditions of very small Reynolds numbers and Grashof numbers.

The present study treats combined forced and free convective heat transfer around a sphere at large Reynolds and Grashof numbers. The analysis encompasses the entire regime of mixed convection, ranging

from pure forced convection to pure free convection. Both aiding and opposing flows, in which the buoyancy force respectively aids and opposes the forced convective flow, are considered. In the analysis, the conservation equations of the boundary layer are transformed such that they can lend themselves to either local nonsimilarity or finite-difference solutions. In the present study, an efficient and very accurate finite-difference method due to Keller and Cebeci [14, 15] is employed to solve the system of transformed equations.

Numerical solutions were carried out and results obtained for gases having a Prandtl number of 0.7, for both aiding and opposing flows. For the aiding flow, the solutions encompassed the range of buoyancy parameter Ω between 0 (pure forced convection) and ∞ (pure free convection). The opposing flow solutions were for Ω between 0 and -3.0.

ANALYSIS

Consider a sphere of radius R which is situated in a flow field with undisturbed oncoming free stream velocity u_∞ and temperature T_∞ as shown in Fig. 3. The convective forced flow is assumed to be moving upward, while the gravity g acts downward in the opposite direction. The surface of the sphere is maintained at a uniform temperature T_w. Let the coordinates be chosen such that x measures the distance along the surface of the sphere from the lower stagnation point and y measures the distance normal to the surface. If $T_w > T_\infty$, the buoyancy force which arises due to the temperature difference will aid the forced flow. On the other hand, if $T_w < T_\infty$, the resulting buoyancy force will oppose the forced flow. The analysis will also be valid for downward flow. In this case, however, the x-coordinate is measured from the upper stagnation point, and the aiding and opposing flows correspond, respectively, to $T_w < T_\infty$ and $T_w > T_\infty$.

In the analysis, it will be assumed that the fluid properties are constant, except that the density variations within the fluid are allowed to contribute to the buoyancy forces. The starting point of the analysis is the following boundary layer equations.

$$\frac{\partial}{\partial x}(ru)+\frac{\partial}{\partial y}(rv)=0, \tag{1}$$

$$u\frac{\partial u}{\partial x}+v\frac{\partial u}{\partial y}=U\frac{\mathrm{d}U}{\mathrm{d}x}+\nu\frac{\partial^2 u}{\partial y^2}+g\beta(T-T_\infty)\sin(x/R), \tag{2}$$

$$u\frac{\partial T}{\partial x}+v\frac{\partial T}{\partial y}=\alpha\frac{\partial^2 T}{\partial y^2} \tag{3}$$

subjected to the boundary conditions

$$\begin{aligned} &u=v=0, \quad T=T_w \text{ at } y=0;\\ &u\to U(x), \quad T\to T_\infty \text{ as } y\to\infty. \end{aligned} \tag{4}$$

In the foregoing equations, the standard symbols are defined in the nomenclature and the radial distance $r(x)$ is given by

$$r=R\sin(x/R). \tag{5}$$

The local free stream velocity $U(x)$ in general has the expression

$$\frac{U}{u_\infty}=A\left(\frac{x}{R}\right)+B\left(\frac{x}{R}\right)^3+C\left(\frac{x}{R}\right)^5+D\left(\frac{x}{R}\right)^7+\ldots \tag{6}$$

from measurements [7], where A, B, C, D, are constants. The corresponding expression from potential flow solution is given by

$$\frac{U}{u_\infty}=\tfrac{3}{2}\sin(x/R) \tag{7}$$

with $A=3/2$, $B=-1/4$, $C=1/80$, $D=-1/3360$, etc. from sine series expansion.

To facilitate a solution, equations (1)–(4) are transformed from the (x, y) coordinates to (ξ, η) coordinates by a proper choice of transformation variables. Since the present study covers the entire regime of mixed convection, with the buoyancy parameter Ω ranging from 0 to ∞, it is convenient to carry out the transformation of the conservation equations separately for forced-flow dominated and buoyancy-force dominated cases. The combination of the solutions from these two cases then encompasses the entire regime of mixed forced and free convection.

Forced-flow dominated case

In this case the buoyancy force is of the secondary importance as compared to the forced convective flow. Thus, the transformation can be patterned after that for pure forced convection such that the buoyancy force effect appears as a parameter. To this end, use is made of Görtler–Meksyn variables given in [16]

$$\xi=\int_0^x\frac{U}{u_\infty}\frac{\mathrm{d}x}{R}, \quad \eta=y\frac{U}{(2\nu R u_\infty\xi)^{1/2}}. \tag{8}$$

It is noted here that ξ is a measure of the dimensionless streamwise coordinate around the surface of the sphere and η is a measure of the dimensionless boundary-layer thickness.

With the introduction of a reduced stream function $f(\xi,\eta)$ and a dimensionless temperature $\theta(\xi,\eta)$

$$f(\xi,\eta)=\frac{\psi(x,y)}{(2\nu R u_\infty\xi)^{1/2}}, \quad \theta(\xi,\eta)=\frac{T(x,y)-T_\infty}{T_w-T_\infty}, \tag{9}$$

where the stream function $\psi(x,y)$ satisfies the continuity equation (1) with

$$u=\frac{1}{r}\frac{\partial}{\partial y}(r\psi), \quad v=-\frac{1}{r}\frac{\partial}{\partial x}(r\psi), \tag{10}$$

equations (1)–(4) can be transformed into the following system of equations:

$$f'''+\gamma(\xi)ff''+\delta(\xi)(1-f'^2)\pm\lambda(\xi)\Omega\theta = 2\xi\left(f'\frac{\partial f'}{\partial\xi}-f''\frac{\partial f}{\partial\xi}\right), \tag{11}$$

$$\frac{1}{Pr}\theta''+\gamma(\xi)f\theta'=2\xi\left(f'\frac{\partial\theta}{\partial\xi}-\theta'\frac{\partial f}{\partial\xi}\right), \tag{12}$$

$$\begin{aligned} &f'(\xi,0)=f(\xi,0)=0, \quad \theta(\xi,0)=1,\\ &f'(\xi,\infty)=1, \quad \theta(\xi,\infty)=0 \end{aligned} \tag{13}$$

in which the primes denote partial derivatives with respect to η,

$$\gamma(\xi) = 1+2\frac{\xi}{U/u_\infty}\frac{\cos(x/R)}{\sin(x/R)},$$

$$\delta(\xi) = 2\xi\frac{\mathrm{d}}{\mathrm{d}\xi}(U/u_\infty)/(U/u_\infty), \qquad (14)$$

$$\lambda(\xi) = 2\frac{\xi\sin(x/R)}{(U/u_\infty)^3}$$

and the buoyancy parameter Ω measures the buoyancy force effects and has the expression

$$\Omega = |Gr|/Re^2 \qquad (15)$$

wherein the Grashof number Gr and the Reynolds number Re are defined, respectively, as

$$Gr = \frac{g\beta(T_w-T_\infty)R^3}{\nu^2}, \quad Re = \frac{u_\infty R}{\nu}. \qquad (16)$$

The plus and minus signs in front of the last term on the LHS of equation (11) refer, respectively, to aiding and opposing flows.

The quantities $\gamma(\xi)$, $\delta(\xi)$, and $\lambda(\xi)$ in equation (14) can be evaluated when the local free stream velocity distribution $U(x)$ is prescribed. For the case of $U(x)$ from the potential flow solution given by equation (7), for example, one can find

$$\gamma = \frac{6-3\xi}{3-\xi}, \quad \delta = \frac{3-2\xi}{3-\xi}, \quad \lambda = \frac{4}{3(3-\xi)}. \qquad (17)$$

At the lower stagnation point ($\xi = 0$), equations (11)–(13) reduce to

$$f''' + 2ff'' + 1 - f'^2 \pm \Omega\theta/A^2 = 0, \qquad (18)$$

$$\frac{1}{Pr}\theta'' + 2f\theta' = 0, \qquad (19)$$

$$f'(0) = f(0) = 0,\ \theta(0) = 1,\ f'(\infty) = 1,\ \theta(\infty) = 0 \qquad (20)$$

where $A = 3/2$ for $U(x)$ both from potential flow solution and from measurements [7].

The physical quantities of primary interest are the velocity distribution $u/U = f'(\xi,\eta)$, the temperature distribution $\theta(\xi,\eta)$, the local friction factor C_f, and the local Nusselt number Nu. The last two quantities are defined, respectively, by

$$C_f = \frac{\tau_w}{\rho u_\infty^2/2}, \quad Nu = \frac{hR}{k}. \qquad (21)$$

From the definitions of wall shear stress $\tau_w = \mu(\partial u/\partial y)_{y=0}$ and local heat-transfer coefficient $h = q_w/(T_w-T_\infty)$, and Fourier's law $q_w = -k(\partial T/\partial y)_{y=0}$, it can be readily shown that

$$C_f Re^{1/2} = (2)^{1/2}[(U/u_\infty)^2/\xi^{1/2}]f''(\xi,0),$$
$$C_f Gr^{1/4} = \Omega^{1/4}C_f Re^{1/2}, \qquad (22)$$

$$NuRe^{-1/2} = -[(U/u_\infty)/(2\xi)^{1/2}]\theta'(\xi,0),$$
$$NuGr^{-1/4} = NuRe^{-1/2}/\Omega^{1/4}. \qquad (23)$$

The corresponding expressions for the stagnation point are

$$C_f Re^{1/2} = 0, \quad NuRe^{-1/2} = -(A)^{1/2}\theta'(0). \qquad (24)$$

Buoyancy-force dominated case

When the buoyancy induced flow dominates over the forced convective flow, one examines the effects of the latter on the former. It is, therefore, appropriate to transform the conservation equations following the pattern that is used for pure free convection. In this connection, one employs the transformation variables

$$X = \frac{x}{R}, \quad Y = \frac{y}{R}|Gr|^{1/4} \qquad (25)$$

along with the reduced stream function $F(X, Y)$ and the dimensionless temperature $\Phi(X, Y)$:

$$F(X,Y) = \frac{\psi(x,y)}{\nu X|Gr|^{1/4}}, \quad \Phi(X,Y) = \frac{T(x,y)-T_\infty}{T_w-T_\infty}. \qquad (26)$$

With the introduction of equations (25) and (26), equations (2)–(4) can be transformed into

$$F''' + \left(1+\frac{X\cos X}{\sin X}\right)FF'' - F'^2 + \sigma(X)\Omega^* + \frac{\sin X}{X}\Phi = X\left(F'\frac{\partial F'}{\partial X} - F''\frac{\partial F}{\partial X}\right), \qquad (27)$$

$$\frac{1}{Pr}\Phi'' + \left(1+\frac{X\cos X}{\sin X}\right)F\Phi' = X\left(F'\frac{\partial\Phi}{\partial X} - \Phi'\frac{\partial F}{\partial X}\right), \qquad (28)$$

$$F'(X,0) = F(X,0) = 0, \quad \Phi(X,0) = 1,$$
$$F'(X,\infty) = \chi(X)\Omega^{*1/2}, \quad \Phi(X,\infty) = 0 \qquad (29)$$

where the primes now stand for partial derivatives with respect to Y,

$$\Omega^* = Re^2/|Gr| = 1/\Omega \qquad (30)$$

and

$$\sigma(X) = [(U/u_\infty)/X]\frac{\mathrm{d}}{\mathrm{d}X}(U/u_\infty),\ \chi(X) = (U/u_\infty)/X. \qquad (31)$$

At the stagnation point, equations (27)–(29) can be simplified to

$$F''' + 2FF'' - F'^2 + A^2\Omega^* + \Phi = 0, \qquad (32)$$

$$\frac{1}{Pr}\Phi'' + 2F\Phi' = 0, \qquad (33)$$

$$F'(0) = F(0) = 0, \quad \Phi(0) = 1,$$
$$F'(\infty) = A\Omega^{*1/2}, \quad \Phi(\infty) = 0. \qquad (34)$$

The streamwise velocity distribution is given by $u/U = [X/(U/u_\infty)]F'(X, Y)/\Omega^{*1/2}$ and the temperature distribution by $\Phi(X, Y)$. The local friction factor C_f and the local Nusselt number Nu as defined by equation (21) now have the expressions

$$C_f Re^{1/2} = 2XF''(X,0)/\Omega^{*3/4},$$
$$C_f Gr^{1/4} = C_f Re^{1/2}/\Omega^{*1/4}, \qquad (35)$$

$$NuRe^{-1/2} = -\Phi'(X,0)/\Omega^{*1/4},$$
$$NuGr^{-1/4} = -\Phi'(X,0). \qquad (36)$$

In the numerical computations, which covered $0 \leqslant \Omega \leqslant \infty$ (i.e. Ω values ranging from pure forced convection to pure free convection), equations (11)–(13) were used for $0 \leqslant \Omega \leqslant 10$ and equations (27)–(29) for $1 \leqslant \Omega \leqslant \infty$ (i.e. $1 \geqslant \Omega^* \geqslant 0$). It was verified that the two sets of equations yielded the same results.

In the numerical results to be presented later, the buoyancy force parameter Ω will be used for the entire regime of mixed convection. It is, therefore, convenient to know the relationships between $F''(X,0)$ and $f''(\xi,0)$ and between $\Phi'(X,0)$ and $\theta'(\xi,0)$. They can be derived from equations (22)–(23) and (35)–(36) to give

$$F''(X,0)=\frac{1}{\sqrt{2}}\frac{(U/u_\infty)^2}{X\xi^{1/2}}\frac{f''(\xi,0)}{\Omega^{3/4}},$$
$$\Phi'(X,0)=\frac{1}{\sqrt{2}}\frac{(U/u_\infty)}{\xi^{1/2}}\frac{\theta'(\xi,0)}{\Omega^{1/4}}. \quad (37)$$

The corresponding equations for the stagnation point are

$$F''(0)=A^{3/2}f''(0)/\Omega^{3/4},\ \Phi'(0)=A^{1/2}\theta'(0)/\Omega^{1/4}. \quad (38)$$

NUMERICAL SOLUTIONS

Solutions of the systems of the partial differential equations (11)–(13) and (27)–(29) were carried out by using a finite-difference method due to Keller and Cebeci [14, 15]. According to this method, equations (11)–(13) [or equations (27)–(29)] are first written in the form of a first-order system by introducing new unknown functions of η-derivatives. The functions and their derivatives in the first-order equations are then approximated by centered difference quotients and averages at the midpoints of net rectangles in the (ξ,η) domain or net segments in the ξ and η coordinates, as required, to yield finite-difference equations with accuracy of the order of $(\Delta\xi)^2$ and $(\Delta\eta)^2$. The resulting nonlinear difference equations, along with the corresponding expressions for the boundary conditions, are finally solved by using Newton's method. The details of the solution method can be found in [14, 15] and are omitted here. However, it needs to be reiterated that this numerical scheme has been shown to be simpler and more flexible and efficient to use than most other numerical methods including the local nonsimilarity method and to provide numerical results of very high accuracy. More importantly, the scheme is numerically stable and thus allows computations to be carried out extremely close to the flow separation point.

RESULTS AND DISCUSSION

Numerical results were obtained for gases having a Prandtl number of 0.7. They cover local wall shear stress, local surface heat-transfer rate, and velocity and temperature distributions for both aiding and opposing flows. The buoyancy force parameter Gr/Re^2 in the computations ranged from 0 (i.e. pure forced convection) to ∞ (i.e. pure free convection with $Re^2/Gr=0$) for aiding flow and from 0 to -3.0 for opposing flow. Since it appears that no experimental information on the local free stream velocity distributions for mixed forced and free convection around a sphere is available, use was made of two expressions from forced convection in the calculations. One of these is the potential flow solution given by equation (7) and the other from the measurements of Frössling [7] as given by equation (6) with $A=1.5$, $B=-0.4371$, $C=0.1481$ and $D=-0.0423$. This latter expression of Frössling is essentially identical to that given by Tomotika and Imai [17] from their experiments and is valid for $x/R\leqslant 1.40$. Thus, the results to be presented will terminate at $\phi=90°$.

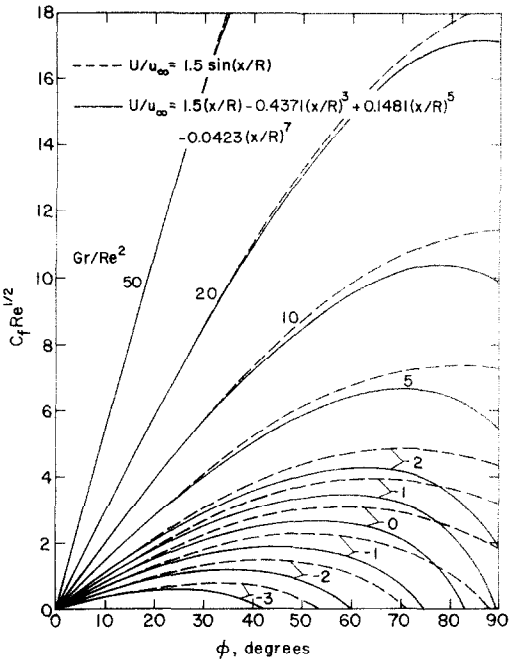

FIG. 1. Angular distributions of the local friction factor, $Pr=0.7$.

Figure 1 illustrates the angular distributions of the local wall shear stress $C_f Re^{1/2}$ for the two local free stream velocity distributions. It can be seen from the figure that the local wall shear increases with increasing buoyancy force for aiding flow ($Gr/Re^2>0$), with a resulting delay in the flow separation. This is because the buoyancy force inside the boundary layer assists the forced flow in acting against the adverse pressure gradient. For the opposing flow case ($Gr/Re^2<0$), on the other hand, the local wall shear is seen to decrease as the buoyancy force increases. As a result, the flow separation occurs earlier and moves toward the stagnation point.

An examination of Fig. 1 reveals that for a given buoyancy force, the local free stream velocity distribution from the potential flow model provides wall shear that is larger than that provided from the experimental measurements of Frössling, with a corresponding delay in the flow separation. This effect is strongly felt for small and moderate buoyancy forces for both aiding and opposing flows, particularly at large angles away from the stagnation point. However, it is interesting to note that for aiding flow with strong buoyancy forces (e.g. $Gr/Re^2\geqslant 20$), the local wall shear tends to become less sensitive to the variation of the local free stream velocity distributions.

The angular distributions of the local Nusselt number $NuRe^{-1/2}$ are shown in Fig. 2. As shown in the figure, the local surface heat-transfer rate increases as the buoyancy force increases for aiding flow, while an

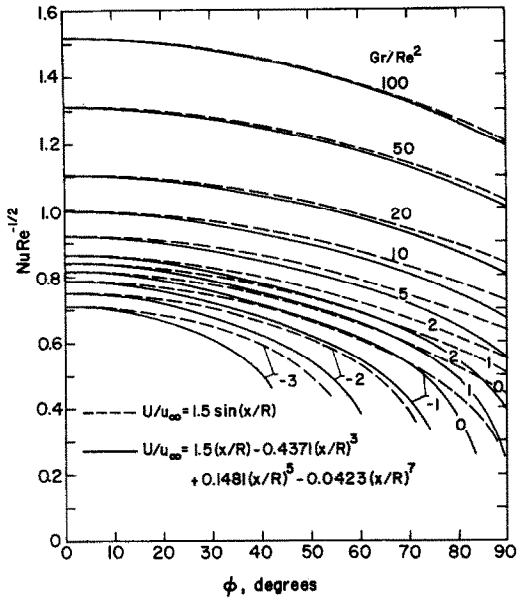

FIG. 2. Angular distributions of the local Nusselt number, $Pr = 0.7$.

opposite trend is observed for opposing flow. Also, for a given buoyancy force, the local Nusselt number is seen to decrease with increasing angle from the stagnation point. As in the wall shear results, Fig. 2 indicates that the local surface heat-transfer results for small to moderate buoyancy forces depend strongly on the variation of the local free stream velocity distributions. For a given buoyancy force, the potential flow velocity distribution is seen to yield local Nusselt number results that are larger than those provided by the measured velocity distribution of Frössling [7]. However, since the measured velocity distribution represents a more realistic flow field outside the boundary layer than the potential flow, the results from the former are believed to be more accurate than those from the latter.

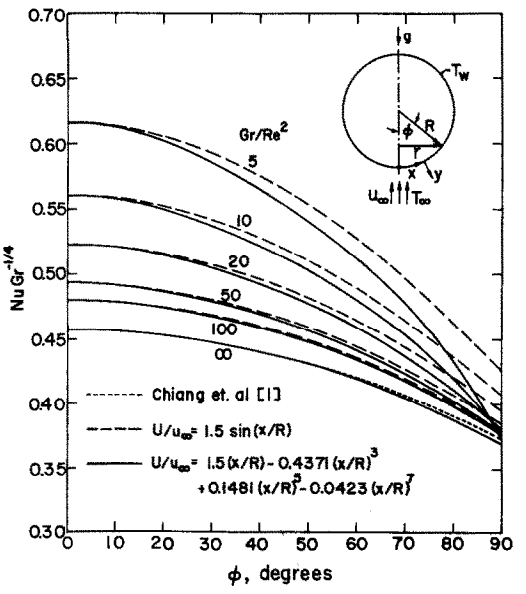

FIG. 3. Angular distributions of the local Nusselt number in terms of $NuGr^{-1/4}$, $Pr = 0.7$.

Figure 3 shows the angular distributions of the local Nusselt number in terms of $NuGr^{-1/4}$ for large buoyancy parameters ($5 \leqslant Gr/Re^2 \leqslant \infty$). The curve for $Gr/Re^2 = \infty$ (i.e. $Re^2/Gr = 0$) corresponds to the case of pure free convection. As to be expected, the effects of the variation of the local free stream velocity distributions on the local Nusselt number diminish completely as Gr/Re^2 increases to ∞. Also included in the figure are the results of Chiang and coworkers [1] for pure free convection, which deviate somewhat from the present results at large angular positions.

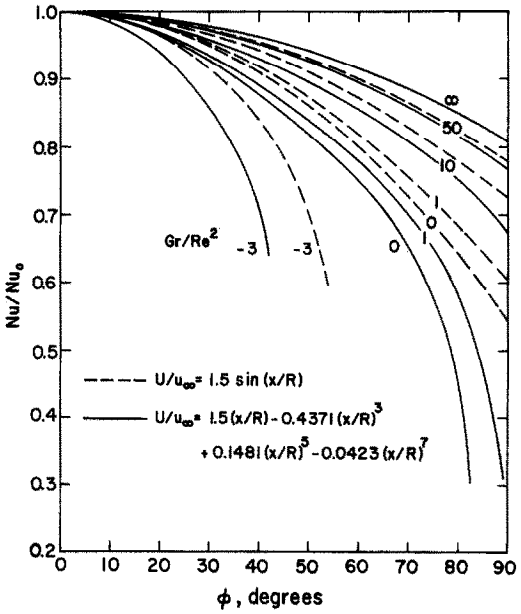

FIG. 4. Relative angular distributions of the local Nusselt number, $Pr = 0.7$.

The relative changes in the local Nusselt number Nu/Nu_0, where Nu_0 is the Nusselt number at the stagnation point, for representative values of Gr/Re^2 are plotted in Fig. 4. As can be seen from the figure, the angular dependence of the local Nusselt number is greater for low to moderate buoyancy forces (i.e. when forced convection is dominant) than for large buoyancy forces (i.e. when free convection is dominant).

To provide a better understanding of the local heat-transfer characteristics for the entire regime of mixed convection for aiding flow, Fig. 5 has been prepared to show the effect of buoyancy forces on the local Nusselt number at three representative angular positions of $\phi = 0$, 60 and 90°. The asymptotes at the stagnation point (i.e. $\phi = 0°$) for pure forced convection ($Gr/Re^2 = 0$) and pure free convection ($Gr/Re^2 = \infty$) are, respectively

$$NuRe^{-1/2} = 0.8149,\quad NuRe^{-1/2} = 0.4576\Omega^{1/4} \quad (39)$$

which agree with the corresponding expressions from previous studies [6, 1]. It should be noted that the curve for the case of $\phi = 90°$ with local free stream velocity distribution from measurements [7] starts from $Gr/Re^2 = 2$. This is because the flow has already separated at $\phi < 90°$ for $Gr/Re^2 < 2$.

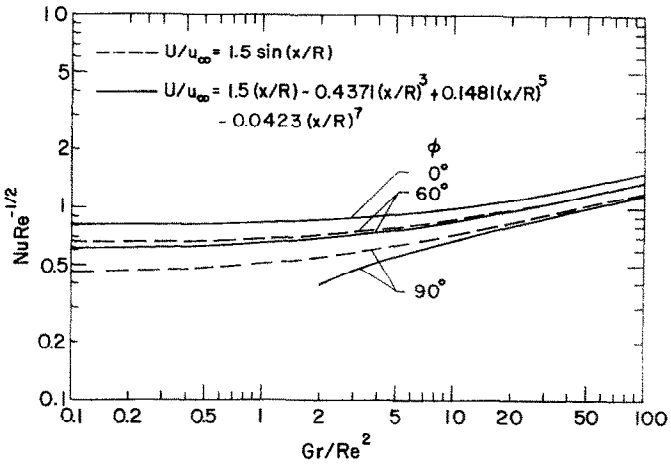

FIG. 5. Heat-transfer results at representative angular positions, $Pr = 0.7$.

It is of practical interest to determine the extent to which the local forced convection Nusselt numbers are affected by the buoyancy forces and the local free convection Nusselt numbers by the inertia forces. This can be most effectively visualized, respectively, in terms of the ratios Nu/Nu_{forced} and Nu/Nu_{free}, where Nu_{forced} and Nu_{free} are the local Nusselt numbers for pure forced and pure free convection, respectively. These ratios for the stagnation point are plotted in Fig. 6 as a function of the buoyancy parameter, with the $Nu_0/Nu_{0,\text{free}}$ curve referring to the upper abscissa scale. The departure of these ratios from unity provides a direct measure of the buoyancy and inertia force effects. If the threshold values of significant buoyancy effects are defined by 5% departures from pure forced convection, the buoyancy effects become significant at $Gr/Re^2 = 1.67$ and -1.33, respectively for aiding and opposing flows. Similarly, with 5% departure from pure free convection ($Re^2/Gr = 0$) as the threshold of significant inertia force effect, the inertia force is found to become important at $Re^2/Gr = 0.01$.

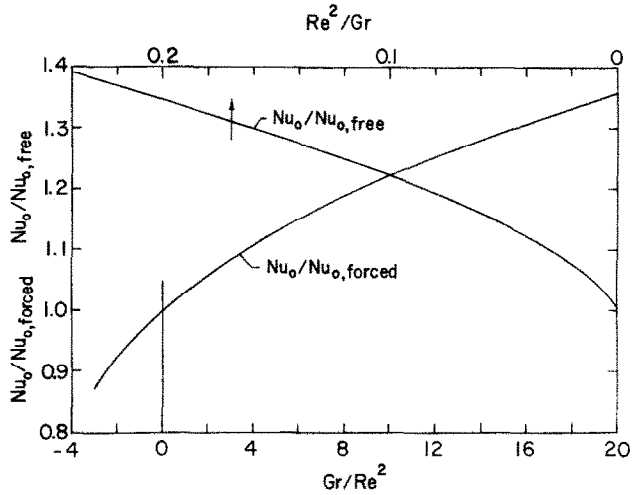

FIG. 6. Effects of buoyancy and inertia forces on the stagnation point heat-transfer results, $Pr = 0.7$.

To illustrate how the buoyancy force affects the velocity and temperature fields in the boundary layer, representative velocity and temperature profiles at the stagnation point for several buoyancy parameters Gr/Re^2 are shown in Figs. 7 and 8, respectively. It is noted that in the figures the dimensionless coordinate $y(u_\infty/\nu R)^{1/2}$ is used as the boundary-layer thickness. It is evident from Fig. 7 that for aiding flow ($Gr/Re^2 > 0$), the velocity gradient at the wall increases as the buoyancy force increases, with an accompanying increase in the velocity near the wall region and an overshooting of the velocity beyond its local free stream value. For the opposing flow ($Gr/Re^2 < 0$), on the other hand, the effect of the buoyancy force is to reduce the velocities compared to those for pure forced convection. As the Gr/Re^2 values become more negative, S-shaped profiles typical of retarded boundary layers are in evidence.

The temperature profiles in Fig. 8 show that for the case of aiding flow, an increase in buoyancy force results in an increase in the temperature gradient at the wall and a decrease in the thermal boundary-layer

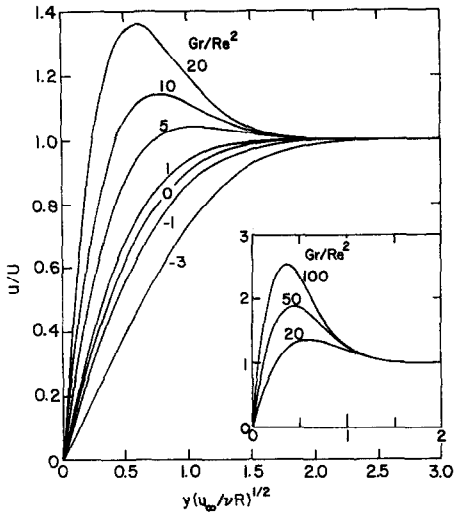

FIG. 7. Representative velocity profiles at the stagnation point, $Pr = 0.7$.

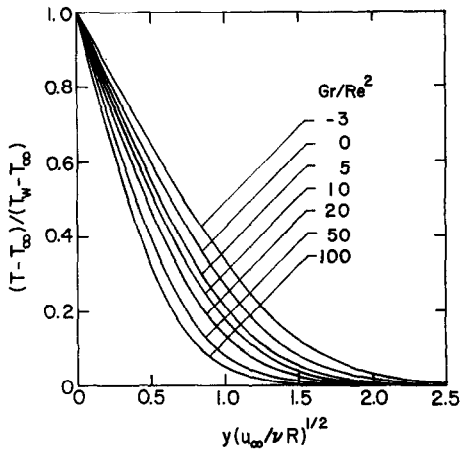

FIG. 8. Representative temperature profiles at the stagnation point, $Pr = 0.7$.

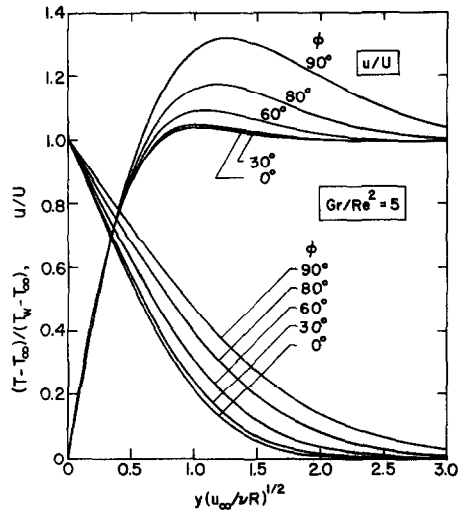

FIG. 9. Velocity and temperature profiles for $Gr/Re^2 = 5$ at representative angular positions, $Pr = 0.7$.

thickness. The opposite trends are in evidence for the case of opposing flow.

Figure 9 illustrates the velocity and temperature profiles for a given buoyancy force parameter of $Gr/Re^2 = 5$ at several angular locations, with the local free stream velocity $U(x)$ from measurements of Frössling [7]. Both the velocity and temperature gradients at the wall are seen to decrease as the angle ϕ increases from 0 to 90°, with a corresponding increase in the flow and thermal boundary-layer thicknesses. A noteworthy behavior in the velocity profiles for a given buoyancy parameter is that whereas the velocity gradient at the wall decreases with increasing angle, the overshooting of the velocity beyond its local free stream value increases as the angle increases. Thus, the velocity profiles cross each other near the wall. The velocity and temperature profiles with $U(x)$ from potential flow solution for the same buoyancy force effect exhibit a pattern similar to that shown in Fig. 9 and are, therefore, omitted here.

It is interesting to compare the present analytical results with those from experiments. For $Gr = 200$, Yuge's empirical formulas for mixed convection from his experiments [11] provided average Nusselt numbers $\overline{Nu}Re^{-1/2}$ of 0.706 and 1.643, respectively for $Gr/Re^2 = 1$ and 50. From the present results in Fig. 2, the local Nusselt number $NuRe^{-1/2}$ is seen to range from 0.841 to 0.486 for $Gr/Re^2 = 1$ and from 1.312 to 1.071 for $Gr/Re^2 = 50$ as ϕ increases from 0° (stagnation point) to 80°. The agreement between the results from analysis and experiments is fair for $Gr/Re^2 = 1$, but is very poor for $Gr/Re^2 = 50$. The discrepancies in the two sets of results are to be expected, because Yuge's experiments were conducted at very low Reynolds and Grashof numbers ($Re = 1.8 \sim 55$, $Gr = 0.125 \sim 230$), whereas the present analysis is based on boundary-layer approximations which are valid only for large Reynolds and Grashof numbers.

CONCLUSIONS

From the results of the present analysis on mixed forced and free convection about a sphere, it is found that for gases having a Prandtl number of 0.7 significant buoyancy force effects on pure forced convection are encountered for $Gr/Re^2 \geqslant 1.67$ and for $Gr/Re^2 \leqslant -1.33$, respectively for aiding and opposing flows. In addition, the inertia force effects on pure free convection are found to be important when $Re^2/Gr \geqslant 0.01$. The local wall shear and local Nusselt number results exhibit a strong dependence on the variation of the local free stream velocities for small to moderate buoyancy forces for both aiding and opposing flows, particularly at large angular positions in the region near the point of flow separation.

Acknowledgements—The present study was supported by a grant from the National Science Foundation (NSF ENG 75-15033).

REFERENCES

1. T. Chiang, A. Ossin and C. L. Tien, Laminar free convection from a sphere, *J. Heat Transfer* **86C**, 537–542 (1964).

2. F. N. Lin and B. T. Chao, Laminar free convection over two-dimensional and axisymmetric bodies of arbitrary contour, *J. Heat Transfer* **96C**, 435–442 (1974).
3. C. J. Cremers and D. L. Finley, Natural convection about isothermal spheres, in *Fourth International Heat Transfer Conference*, Paris–Versailles, Vol. 4, Paper No. NC 1.5. Elsevier, Amsterdam (1970).
4. A. A. Kranse and J. Schenk, Thermal free convection from a solid sphere, *Appl. Scient. Res.* **A15**, 397–403 (1966).
5. B. T. Chao and R. O. Fagbenle, On Merk's method of calculating boundary layer transfer, *Int. J. Heat Mass Transfer* **17**, 223–240 (1974).
6. H. L. Evans, *Laminar Boundary-Layer Theory*, Chapter 9. Addison-Wesley, Reading, MA (1968).
7. N. Frössling, Evaporation, heat transfer, and velocity distribution in two-dimensional and rotationally symmetrical laminar boundary-layer flow, National Advisory Committee for Aeronautics, TM 1432 (1958).
8. G. C. Vliet and G. Lepper, Forced convection heat transfer from an isothermal sphere to water, *J. Heat Transfer* **83C**, 163–175 (1961).
9. J. R. Cary, The determination of local forced-convection coefficients for spheres, *Trans. Am. Soc. Mech. Engrs* **75**, 483–487 (1953).
10. D. H. Baer, W. G. Schlinger, V. J. Berry and B. H. Sage, Temperature distribution in the wake of a heated sphere, *J. Appl. Mech.* **20**, 407–414, *Trans. Am. Soc. Mech. Engrs* **75** (1953).
11. T. Yuge, Experiments on heat transfer from spheres including combined natural and forced convection, *J. Heat Transfer* **82C**, 214–220 (1960).
12. L. S. Klyachko, Heat transfer between a gas and a spherical surface with the combined action of free and forced convection, *J. Heat Transfer* **85C**, 355–357 (1963).
13. C. A. Hieber and B. Gebhart, Mixed convection from a sphere at small Reynolds and Grashof numbers, *J. Fluid Mech.* **38**, 137–159 (1969).
14. H. B. Keller and T. Cebeci, Accurate numerical methods for boundary-layer flows. II: Two-dimensional turbulent flows, *AIAA Jl* **10**, 1193–1199 (1972).
15. T. Cebeci, Laminar free convective heat transfer from the outer surface of a vertical slender circular cylinder, *Proceedings of the 5th International Heat Transfer Conference, Tokyo, Japan*, Vol. 3, pp. 15–19. Japan Soc. Mech. Engrs and Soc. Chem. Engrs (Japan), Tokyo (1974).
16. E. M. Sparrow, H. Quack and C. J. Boerner, Local nonsimilarity boundary-layer solutions, *AIAA Jl* **8**, 1936–1942 (1970).
17. S. Tomotika and I. Imai, On the transition from laminar to turbulent flow in the boundary layer of a sphere, *Rep. Aeronaut. Res. Inst., Tokyo*, Vol. 13, 389–423 (1938).

ANALYSE DE LA CONVECTION MIXTE AUTOUR D'UNE SPHERE

Résumé—On étudie l'écoulement et le transfert thermique par convection naturelle ou forcée autour d'une sphère. Les équations de conservation des couches limites sont résolues par une méthode de différences finies. On présente les résultats numériques pour des gaz ayant un nombre de Prandtl égal à 0,7 et des paramètres qui couvrent tout le régime de la convection mixte, depuis la convection forcée pure jusqu'à la convection naturelle pure. On trouve que le facteur local de frottement et le nombre de Nusselt local augmentent lorsque les forces d'Archimède aident l'écoulement et décroissent dans le cas contraire. On examine les effets de la variation des vitesses locales de l'écoulement libre, sur le frottement pariétal et le transfert thermique. Les effets des forces d'Archimède sur la convection forcée deviennent significatifs pour $Gr/Re^2 > 1{,}67$ et $< -1{,}33$ respectivement pour les écoulements en cocourant ou en opposition. Les effets des forces d'inertie sont significatifs pour $Re^2/Gr > 0{,}01$. Les profils de vitesse montrent un dépassement de la vitesse de l'écoulement libre pour le cas favorable et une forme en S pour le cas de l'opposition.

UNTERSUCHUNG DER GEMISCHTEN ERZWUNGENEN UND FREIEN KONVEKTION OBERHALB EINER KUGEL

Zusammenfassung—Es werden die Strömungs- und Wärmeübergangsverhältnisse bei laminarer, gemischter erzwungener und freier Konvektion oberhalb einer Kugel untersucht. Die transformierten Erhaltungsgleichungen für die nicht ähnlichen Grenzschichten werden mit Hilfe eines Differenzenverfahrens gelöst. Für Gase mit $Pr = 0{,}7$ und Auftriebsparameter, die den gesamten Bereich der gemischten Konvektion von der reinen erzwungenen bis zur reinen freien Konvektion umfassen, werden numerische Ergebnisse angegeben. Im allgemeinen ergibt sich, daß der örtliche Widerstandsbeiwert und die örtliche Nusselt–Zahl mit zunehmenden Auftriebskräften bei gleichgerichteter Strömung zunehmen, bei entgegengesetzter Strömung abnehmen. Der Einfluß der Aenderung der örtlichen Anströmgeschwindigkeiten auf die Wandschubspannungen und den Wärmeübergang wird ebenfalls untersucht. Der Wärmeübergang bei erzwungener Konvektion wird merklich beeinflußt durch die Auftriebskräfte bei $Gr/Re^2 > 1{,}67$ für gleichgerichtete Strömung, bzw. $Gr/Re^2 < -1{,}33$ für entgegengerichtete Strömung. Der Einfluß der Trägheitskräfte auf die freie Konvektion ist für $Re^2/Gr > 0{,}01$ von Bedeutung. Bedingt durch den Auftrieb werden die Geschwindigkeitsprofile verändert; bei gleichgerichteter Strömung werden die örtlichen Anströmgeschwindigkeiten überschritten, bei entgegengesetzter Strömung ergibt sich ein S-förmiger Verlauf.

ИССЛЕДОВАНИЕ СМЕШАННОЙ ВЫНУЖДЕННОЙ И ЕСТЕСТВЕННОЙ КОНВЕКЦИИ ОКОЛО СФЕРЫ

Аннотация — Проведено исследование характеристик потока и теплообмена при ламинарной смешанной вынужденной и естественной конвекции около сферы. Преобразование уравнения сохранения для неавтомодельных пограничных слоев решалось с помощью конечно-разностного метода. Численные результаты для газов с числом Прандтля, равным 0,7, представлены для широкого диапазона свободноконвективных параметров, характеризующих весь режим смеанной конвекции от чисто вынужденной до чисто естественной. Найдено, что в общем случае шлокальный коэффициент трения и локальное число Нуссельта увеличиваются с увеличением

подъемной силы при спутном течении и уменьшаются с ее увеличением в случае противотока. Исследовалось также влияние локальных скоростей невозмущенного потока на пристенный сдвиг и теплообмен на поверхности. Как показывают данные по теплообмену, влияние подъемной силы на вынужденную конвекцию становится значительным при $Gr/Re^2 > 1{,}67$ и $< -1{,}33$ для спутного потока и противотока. Найдено, что влияние силы инерции на свободную конвекцию существенно при $Re^2/Gr > 0{,}01$. Скоростные профили, на которые оказывает влияние подъемная сила, показывают отклонение от локальной скорости свободного течения в случае спутного потока и имеют S-образную форму для противотока.